Restricted role of experiments in real space in determination of the Si(111)7×7 reconstructed structure

Tsuyoshi Yamaguchi
Faculty of Engineering, Shizuoka University, Hamamatsu 432, Japan
(Received 28 January 1985)

Atomic displacements for the Si(111)7×7 reconstructed structure are calculated for five models which are consistent with scanning tunneling microscopy, an experiment in real space. They are (1) the adatom model, (2) the adatom π-bond model, (3) the adatom stacking-fault model, (4) the adatom stacking-fault π-bond model, and (5) the adatom double-stacking-fault model. The unreconstructed structures of these models do not explain very well the results of low-energy ion scattering spectroscopy, another experiment in real space. The reconstructed structures of all models give better results. All give similar spectra to those of the "pyramidal" model, which has been asserted to be the best explanation of experiment. The reconstructed adatom stacking-fault model gives perhaps the best spectra. However, at this stage, the best model really cannot be determined using only ion scattering spectroscopy, because the experimental spectra have broad peaks. It is hoped that further ion scattering work will show fine structure or that a third experiment in real space will be done in the near future.

I. INTRODUCTION

It was a notable advance when Binnig *et al.*[1] proposed the adatom model of the Si(111)7×7 structure by performing scanning tunneling microscopy, the first experiment in real space. They determined the scattering center in experiments in **k** space to have an adatom-like center. The adatom model[1] has 12 adatoms in the 7×7 unit cell, leaving 13 dangling bonds; the total number of dangling bonds is 25. At the corner of the cell, there is no adatom. The atomic arrangement has mirror symmetry with respect to the long diagonal of the cell and threefold-rotational symmetry at the corner.

Aono *et al.*[2] performed low-energy He^+-ion scattering, another experiment in real space. They revealed that the adatom model without atomic displacement could not explain their results and proposed the "pyramidal" model. However, the surface energy of this model seems to be very high, as the number of dangling bonds is 97.

The author[3] extended the adatom model[1] and took into account the displacement of atoms. The adsorption of adatoms reduces the number of dangling bonds but gives rise to atomic displacements. The calculated atomic displacements are very large. The adatoms, for example, shift upward by almost 50% of the layer distance of 0.784 Å. Even the third-layer atoms shift by more than 25% of the layer distance. The new ion scattering spectra are improved from those of the unreconstructed adatom model. They are now close to those of the pyramidal model,[2] which was previously asserted to be the best model for explaining the results of ion scattering.

McRae and Petroff[4] and Takayanagi *et al.*[5] performed transmission electron diffraction spectroscopy. They claim that even our reconstructed adatom model[3] does not completely explain the diffraction pattern, although it gives an improved pattern. Takayanagi *et al.*[5] proposed the adatom stacking-fault model described later.

We believe that reliable models of the Si(111)7×7 structure should explain the two experiments in real space and also experiments in **k** space. Note that the adatom-related models given below explain the gross feature of the scanning tunneling microscopy and many experiments in **k** space. So, it is important to investigate the ion scattering spectra of these models.

In this paper we calculate the atomic displacement of five adatom-related models: (1) the adatom model (AM) of Binnig *et al.*,[1] (2) the adatom π-bond model (APM) of Chadi,[6] (3) the adatom stacking-fault model (ASM) of Takayanagi *et al.*,[5] (4) the adatom stacking-fault π-bond model (ASPM), and (5) the adatom double-stacking-fault model (ADM) of Bennet.[7] We compare the calculated ion scattering spectra of these reconstructed models with experiment.

Note that McRae and Petroff[4] proposed another adatom-related model, the adatom triangle-dimer model, wherein the number of dangling bonds is 73 $(3\times12+18+18+1)$. Furthermore, the dimerization gives rise to atomic displacements. As the surface energy of this model seems to be very high, we do not consider it in this paper.

II. RECONSTRUCTED STRUCTURE AND ION SCATTERING SPECTRA

Taking Keating's model,[8] we express[3] the surface energy due to atomic displacement as

$$E=\alpha\sum_{\substack{\text{all}\\\text{bonds}}}(\mathbf{X}_{ij}^2-3a^2/8)^2+\beta\sum_{\substack{\text{all}\\\text{bonds}\\\text{pairs}}}(\mathbf{X}_{ij}\cdot\mathbf{X}_{jk}+a^2/8)^2\,, \quad (1)$$

for the crystal with the diamond structure where each atom has an electron configuration sp^3. The first and second terms represent bond-stretching and bond-bending interactions between nearest-neighbor atoms, respectively. α and β denote the corresponding force constants. $\mathbf{X}_{ij}$

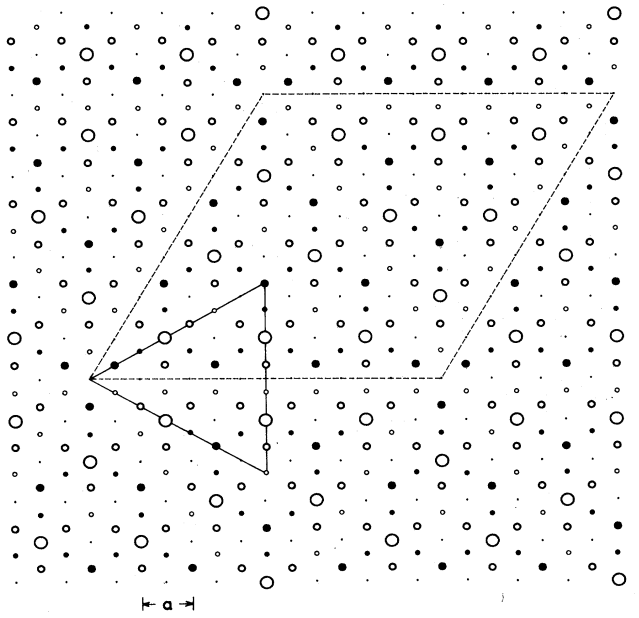

FIG. 1. The 7×7 and our unit cells of the adatom model (AM) represented by dashed and solid lines, respectively. Our cell is bounded by the mirror-symmetry lines with respect to the long diagonal of the real cell. The first-, second-, third-, and fifth-layer atoms are represented by circles with diameters which become smaller for deeper atoms. The fourth-, sixth-, seventh-, and eighth-layer atoms are hidden behind the third-, fifth-, second-, and seventh-layer atoms, respectively. There are also the fifth-layer atoms behind the first-layer atoms. Solid circles show atoms in the reconstructed AM which do not shift from the positions in the unreconstructed AM.

$(=\mathbf{X}_i-\mathbf{X}_j)$ is a relative atomic displacement and a $(=3.84$ Å$)$ is the lattice constant of the unreconstructed surface. We allow coordinates up to the seventh-layer atoms to change, therefore minimizing Eq. (1) and determining the reconstructed structures of five models.

We assume[3] that the arrangement of atoms in the reconstructed structure has the same symmetry properties as in the unreconstructed structure, namely mirror symmetry with respect to the long diagonal of the unit cell and threefold-rotational symmetry at the corner of the cell. Being that there are three inequivalent cells, as shown in Fig. 1, our unit cell is an equilateral triangle, the area of which is one-sixth that of the real unit cell. The number of degrees of freedom becomes a number manageable in computer calculation.

As shown later, the relaxation of adatoms is large. It is necessary to use many anharmonic terms higher than those of the Keating model[8] for surface atoms. There is, however, no experimental or theoretical work from which we can obtain the interaction constants. Assuming that the atomic displacements decay exponentially for bulk atoms, we take[3] the bond length as

$$(\sqrt{3}a/2\sqrt{2})[1+b\exp(-z/z_0)]\ , \qquad (2)$$

where b and z_0 are additional fitting parameters, and z is the distance of the center of the bond from the surface.

In our previous work,[3] we fixed the ratio of force constants to be that of the bulk, $\beta/\alpha=0.29$.[8] In this paper, changing the value of the ratio,[9] we derive the reconstructed structures of various models and their ion scattering spectra.

In ion scattering spectroscopy,[2] no incident ions can penetrate into the shadow cone of any surface atom. The shape of the shadow cone can be described by the Thomas-Fermi-Moliere potential. As we change the ion incidence direction from parallel to normal to the surface, the intensity of ion scattering increases stepwise. Due to the ion-neutralization effect, the intensity of the scattering by a deeper atom, which is outside of the shadow cone of any surface atom, decreases exponentially as a function of the depth from the surface. The spectra in this paper indicate the number of visible atoms which are out of any shadow cone; however, this number is weighted by the ion-neutralization factor.

In the unreconstructed structure, many pairs of atoms take the same relative positions. The ion scattering intensity is a step function with abrupt jumps. In the reconstructed structure, however, the intensity does not change abruptly but changes only gradually due to the large displacements of surface atoms. The resultant spectra show a steep increase at low angles but a rather gentle increase at high angles. The calculation shows that atoms of three surface layers mainly determine the spectra.

As no ions penetrate into the shadow cone, the ion-flux density is high near the shadow cone, and decreases exponentially and becomes constant far outside the shadow cone. This focusing effect[2] makes the spectrum diverge at

TABLE I. Strain energy per 7×7 unit cell of the adatom model (AM), the adatom π-bond model (APM), the adatom stacking-fault model (ASM), the adatom stacking-fault π-bond model (ASPM), and the adatom double-stacking-fault model (ADM). The bond-stretching constant is assumed to have the same value as the bulk α_0. If the surface is softened or hardened, we should multiply the values tabulated by the ratio of bond-stretching constants of the surface and the bulk α/α_0. For comparison, the strain energy per 7×7 cell of the π-bond chain model of the Si(111)2×1 structure is also given.

	$\beta/\alpha=0.29$ (eV)	$\beta/\alpha=0.4$ (eV)
Unreconstructed AM	95.86	132.22
Reconstructed AM	77.39	104.76
Unreconstructed APM	152.86	197.94
Reconstructed APM	95.23	114.15
Unreconstructed ASM	111.19	151.81
Reconstructed ASM	89.30	120.87
Unreconstructed ASPM	141.78	187.57
Reconstructed ASPM	97.12	131.09
Unreconstructed ADM	107.74	146.58
Reconstructed ADM	82.31	110.92
Unreconstructed Si(111)2×1	121.92	165.07
Reconstructed Si(111)2×1	28.77	36.15

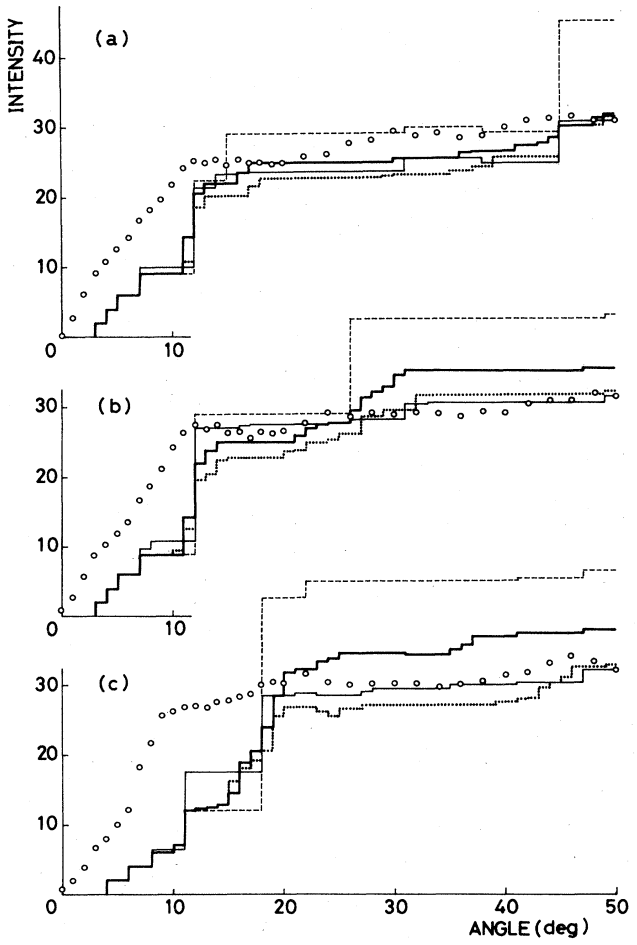

FIG. 2. Intensity of He^+-ion scattering spectroscopy for AM. The dashed, dotted, thick solid, and thin solid lines and the small circles show the spectra of the unreconstructed AM, the reconstructed AM with $\beta/\alpha=0.29$ and 0.4, the pyramidal model, and the experiment, respectively. The experimental spectrum is normalized to the pyramidal model at 50°. Here, the angle of the ion direction of incidence is measured from the surface. (a) Spectrum A in the notation of Aono *et al.*; the azimuthal angle of the ion direction of incidence is along the $[\bar{1}2\bar{1}]$ direction of the long diagonal of the unit cell. (b) Spectrum B; the azimuthal angle is along the $[1\bar{2}1]$ direction. (c) Spectrum C; the azimuthal angle is along the short diagonal.

critical angles where the intensity changes stepwise and makes it decrease exponentially above the critical angles. Furthermore, the surface atoms vibrate at the temperature at which the 7×7 structure is realized. This vibration effect makes the peaks of the spectrum broad.

In this paper we consider only the first two effects, shadowing and ion neutralization. We calculate the atomic displacement of the adatom-related models. If we obtain spectra similar to those of the pyramidal model,[2] then the final spectra, which can be obtained by phenomenologically taking[2] into account the last two effects, focusing and vibration, will be closer to experiment.

A. The adatom model

Figure 1 shows the atomic arrangement[1] of this model. Atoms of the nth layer are at the $A,B,C,C,A,A,B,B,\ldots$ sites for $n=1,2,3,\ldots$. The 7×7 unit cell has 25 dangling bonds. For $\beta/\alpha=0.29$ (the value of the bulk), the atomic arrangement and the ion scattering spectra of the reconstructed AM are given in Ref. 3. The strain energy, bond parameters, and the calculated ion scattering spectra are shown in Tables I and II, and by dotted lines in Fig. 2, respectively, to compare with the results of other models. Note that the bond length for surface-layer atoms is smaller than that of the bulk. For $\beta/\alpha=0.4$ (the expected value of the surface[9]), the atomic arrangement is given in Ref. 9. Bond angles of surface-layer atoms are given in Table III. The unreconstructed AM has nine highly strained bond angles per adatom, three 180° and six 70.73° bond angles. In the reconstructed AM they are around 165° and 80°, respectively.

The newly calculated ion scattering spectra for $\beta/\alpha=0.4$ are shown by thick solid lines in Fig. 2. Here we take the intensity of scattering by the top adatom as unity. We see that the spectra for $\beta/\alpha=0.4$ are not much different from those for $\beta/\alpha=0.29$; if we normalize these spectra to the experimental spectra at 50°, they are similar to each other. However, they are much better than those of the unreconstructed AM (Ref. 1) shown by dashed lines. They are close to those of pyramidal model of Aono *et al.*[2] shown by thin lines.

For spectrum A in the unreconstructed AM shown in Fig. 2, nine adatoms are visible at angles above 7°. The remaining three adatoms and 28 second-layer atoms become visible at 12°, nine second-layer atoms at 15°, and 12 second- and 49 third-layer atoms at 45°. This causes the

TABLE II. Bond parameters defined by the bond length $(\sqrt{3}a/2\sqrt{2})[1+b\exp(-z/z_0)]$ [see Eq. (2) of the text]. The infinite value of z_0 means that the bond length does not decay exponentially up to the eighth-layer atoms considered here.

	$\beta/\alpha=0.29$		$\beta/\alpha=0.4$	
	b	z_0	b	z_0
AM	−0.04273	0.18415a	−0.05034	0.21048a
APM	0.00759	∞	0.00774	∞
ASM	0.01813	4.0054a	0.01174	25.435a
ASPM	0.02077	3.8072a	0.01616	5.2234a
ADM	0.00991	5.8642a	0.00772	10.074a
Si(111)2×1	−0.00179	0.0042a	0.03281	1.2463a

TABLE III. Bond angles for surface-layer atoms of the adatom model (AM) and the number of bonds in the 7×7 unit cell.

Layer	Unreconstructed (deg)	Number of bonds	$\beta/\alpha=0.29$ (deg)	$\beta/\alpha=0.4$ (deg)
1-2-3	180	3×12	164.9—171.8	164.3—171.0
	70.53	6×12	79.23—83.01	79.74—83.35
2-1-2	109.47	3×12	98.65—103.0	98.72—102.4
2-3-2	109.47	3×49	94.28—119.4	93.66—119.9
2-3-4	109.47	3×49	98.90—114.8	98.38—114.7

stepwise increase of the ion scattering intensity. For spectrum *B*, nine adatoms are visible at angles above 7°, three adatoms and 37 second-layer atoms at angles above 12°, 12 second- and 37 third-layer atoms at angles above 26°, and 12 third-layer atoms at angles above 60°. For spectrum *C*, 12 adatoms are visible at angles above 12°, 49 second- and 37 third-layer atoms at angles above 18°, and 12 third-layer atoms at angles above 22°.

In the reconstructed AM,[3] the scattering intensity at low angles remains almost the same as that of the unreconstructed AM but increases continuously at high angles. However, the order of atoms which become visible as we increase the incidence angle remains the same as that of the unreconstructed AM.

Our calculation shows that for any value of β/α, 13 second- and 27 third-layer atoms remain[10] in the same place as in the unreconstructed AM. These atoms, denoted by solid circles in Fig. 1, also contribute to the ion scattering. Physically, for large β/α our system prefers bond angles closer to 109.5° for the sp^3 atoms. Thus, the upward shift of adatoms is smaller for large β/α, as shown in Table I of Ref. 3 and Table III of Ref. 9. If we take the intensity of scattering by the top adatom as unity, the contribution of the second- and third-layer atoms to the scattering becomes larger. As deeper atoms become visible at high angles, the scattering intensity for large β/α becomes larger at high angles, as shown in Fig. 2.

B. The adatom π-bond model

Chadi[6] has proposed a new adatom model, shown in Fig. 3. His model involves a rebonding of a dangling-bond-site atom of the second layer of the AM to the fourth-layer atom as in the π-bond chain model of the Si(111)2×1 structure by Pandey.[11] The dangling-bond-site atom becomes fourfold coordinated by becoming a third-layer atom bonded to a fourth-layer atom, and the third-layer atom becomes a threefold-coordinated second-layer atom. The segmented line in Fig. 3 show schematically the reversal of the coordinations of dangling-bond-site atoms and third-layer atoms. This rebonding gives rise to further atomic displacements. Note that the number of dangling bonds is 25 and the same as that of the AM.

Chadi[6] takes 159 atoms consisting of twelve adatoms, 49 second- and 49 third-layer Si atoms, and 49 H atoms. He performs a force-and-energy minimization using an empirical tight-binding method. He shows that the rebonding reduces the 180° bond angles in AM to around 160°. These bond angles in the reconstructed APM are around 134°. Furthermore, he shows that the adatoms on the two halves of the unit cell differ in their heights relative to a reference (111) plane by about 20% of the layer distance $a/2\sqrt{6}$, 0.784 Å.

Atomic arrangement according to our calculation is given in Table IV. Atoms near a rebonded pair shift more than others. The former shifts more for large β/α and the latter shifts nearly the same for any value of β/α. The adatoms on the two halves of the unit cell differ in their heights by 23.6% of the layer distance for $\beta/\alpha=0.29$ and 35.4% for $\beta/\alpha=0.4$. The shift is small for deeper atoms apart from the rebonded pair but large for atoms near the rebonded pair. Even the fourth-layer atom just below the rebonded pair shifts by $0.1628a$ for $\beta/\alpha=0.29$, the fifth-layer atom by $0.1219a$, and the sixth-layer atom by $0.0605a$. Near the rebonded pair of the unreconstructed APM there are four bonds with length $0.943l$ and a bond with length $1.374l$, where l is the bond length of the bulk $\sqrt{3}a/2\sqrt{2}$. In the recon-

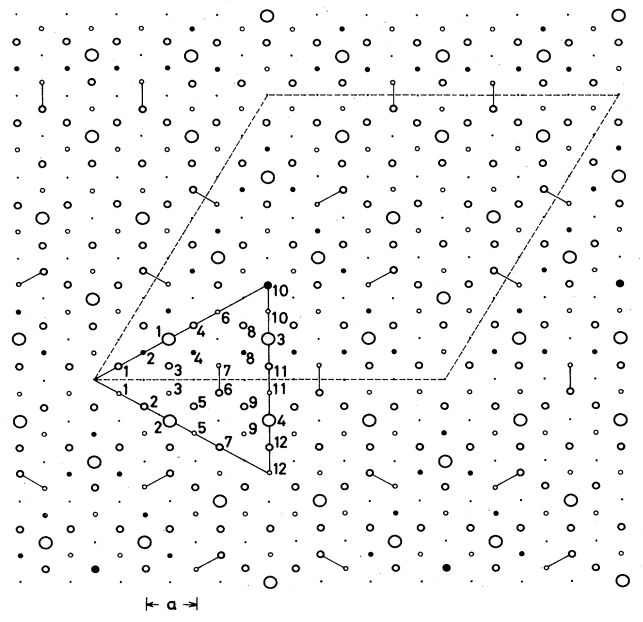

FIG. 3. The same for the adatom π-bond model (APM) as in Fig. 1. The segmented line shows schematically the reversal of bonding of the second- and third-layer atoms of AM as in the π-bond chain model of the Si(111)2×1 structure. Solid circles show atoms in the reconstructed APM which do not shift from the positions in the unreconstructed APM.

TABLE IV. Magnitude and direction of the shift of atoms in the first, second, and third layers of the adatom π-bond model (APM) with the ratio of interaction constants $\beta/\alpha=0.29$ and 0.4. Direction denoted by azimuthal angle with an asterisk (*) is fixed in the calculation. Atoms in the second and third layers which are not tabulated here do not shift.

		$\beta/\alpha=0.29$			$\beta/\alpha=0.4$		
Layer	Atom	Magnitude	Polar angle (deg)	Azimuthal angle (deg)	Magnitude	Polar angle (deg)	Azimuthal angle (deg)
1	1	0.14924a	5.36	30.0*	0.14973a	5.27	30.0*
	2	0.20099a	5.07	150.0*	0.22440a	7.47	150.0*
	3	0.15535a	6.07	90.0*	0.15784a	3.68	90.0*
	4	0.19948a	1.76	−90.0*	0.22930a	8.83	−90.0*
2	1	0.03207a	17.7	30.0*	0.03894a	19.4	30.0*
	2	0.07450a	41.2	−30.0*	0.08015a	35.9	−30.0*
	3	0.06949a	53.9	85.8	0.07085a	56.6	86.3
	4	0.05572a	39.8	−150.0*	0.05863a	39.5	−150.0*
	5	0.10154a	29.7	−169.9	0.12086a	31.2	−156.7
	6	0.17786a	10.8	90.0	0.23163a	7.60	−92.3
	7	0.01284a	31.4	150.0*	0.01023a	31.1	150.0*
	8	0.06025a	43.0	−30.6	0.06494a	43.3	−38.8
	9	0.09776a	29.3	−3.38	0.12280a	30.2	−28.8
	11	0.07973a	52.9	90.0*	0.07748a	52.7	90.0*
	12	0.07786a	42.3	90.0*	0.07867a	34.6	90.0*
3	1	0.07606a	27.9	−30.0*	0.08281a	25.2	−30.0*
	3	0.06511a	50.2	85.5	0.06897a	44.7	79.6
	5	0.04236a	19.5	150.0*	0.04205a	16.2	150.0*
	6	0.10363a	2.12	30.0*	0.10915a	1.66	30.0*
	7	0.0	none	none	0.12454a	80.1	−90.0
	9	0.03391a	42.1	110.3	0.02921a	23.9	106.0
	10	0.0	none	none	0.00142a	0.0	0.0
	11	0.08054a	53.3	90.0*	0.08390a	39.2	90.0*
	12	0.11687a	0.0*	0.0*	0.12366a	0.0*	0.0*

structed APM, the former has length $0.943l-1.057l$ and $1.040l-1.058l$ for $\beta/\alpha=0.29$ and 0.4, respectively, and the latter has length $1.115l$ and $1.088l$.

Bond angles are given in Table V. The 160.53° bond angles in the unreconstructed APM are around 141° and 137° for $\beta/\alpha=0.29$ and 0.4, respectively. These bond angles are nearly equal to those obtained by Chadi.[6] Thus, the APM has the advantage that twelve 180° bond angles

TABLE V. The same for APM as Table III.

Layer	Unreconstructed (deg)	Number of bonds	$\beta/\alpha=0.29$ (deg)	$\beta/\alpha=0.4$ (deg)
1-2-2	160.53	2×6	141.4–141.9	137.2
1-2-3	180.0	(3 + 1)×6	159.3–169.2	156.8–167.3
	70.53	6×12	80.81–86.52	81.11–88.56
2-1-2	109.47	3×12	92.62–98.18	91.01–98.33
2-2-2	120.0	1×6	116.5	121.5
2-2-3	118.13	(2 + 4)×6	109.6–118.0	102.2–115.8
2-3-2	109.47	3×49−7×6	92.87–115.6	90.09–116.7
2-3-3	118.13	(2 + 4)×6	114.2–122.1	112.5–127.4
2-3-4	109.47	3×49−5×6	103.0–114.8	102.8–116.5
	66.16	1×6	84.27	97.76
3-2-3	109.47	3×49−7×6	102.2–121.0	103.3–120.0
3-3-3	120.0	1×6	120.0	101.0
3-3-4	110.06	2×6	108.5–109.5	108.3
	90.0	2×6	91.61–92.27	94.01–94.25
3-4-5	152.78	1×6	149.1	140.6
	109.47	3×49−3×6	104.6–114.0	106.0–113.5
	85.36	2×6	98.77–99.52	99.74–99.89

of the first-, second-, and third-layer atoms are reduced to around 140°, and that the adatoms on the two halves of the cell differ in their heights. However, the APM has the disadvantage that bond angles for deeper atoms near a rebonded pair are quite different from 109.47°. For example, the unit cell of the unreconstructed APM has six 66.16°, 12 90°, six 152.78° and 12 85.36° bond angles for deeper atoms. These are not taken into account by Chadi.[6] As shown in Table I, the strain energy of the APM is 1.23 times higher than that of the AM for $\beta/\alpha=0.29$ and 1.09 times higher for $\beta/\alpha=0.4$.

The ion scattering spectra are shown in Fig. 4. The unreconstructed APM does not explain the experiment[2] and the reconstructed APM gives spectra which are close to those of the pyramidal model. The spectra for $\beta/\alpha=0.29$ are closer than those for $\beta/\alpha=0.4$.

Physically, as large values of β/α prefer bond angles close to 109.47°, the rebonding causes larger displacement of adatoms for large β/α, as in Table IV. Furthermore, one second- and 15 third-layer atoms do not shift from the positions in the unreconstructed APM. As in Sec. II A, we see that the ion scattering intensity becomes small at high angles for large β/α.

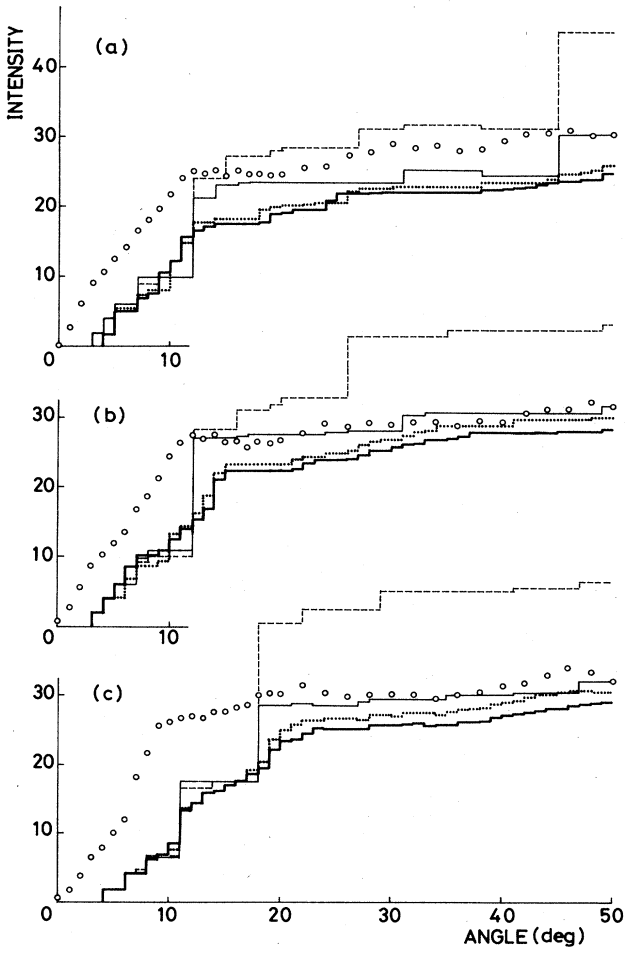

FIG. 4. The same for APM as in Fig. 2.

C. The adatom stacking-fault model

Takayanagi *et al.*[5] have obtained the potential distribution in real space by taking the inverse Fourier transform of the structure factor of their transmission-electron diffraction pattern. They have proposed the model described below.

The atomic arrangement of their ASM is shown in Fig. 5. The arrangement of adatoms is the same as in the AM; adatoms are at the *A* site. The second-layer atoms on the lower-left and upper-right halves of the real unit cell are at the *C* and *B* site, respectively. Atoms from the third layer are at the *A*, *A*, *C*, *C*, *B*, and *B* sites for either half of the cell. There are stacking faults along borders of a triangular subunit (the sides and the short diagonal of the unit cell). The third-layer atoms on the lines of stacking faults shift laterally by $a/6$ and pairs of neighboring atoms rebond with each other. Its bond length is $2a/3$. There is a deep hole at the corner of the cell. The arrangement of the first- through fourth-layer atoms has mirror symmetry with respect to the borders of the triangular subunit. As the ion scattering intensity is mainly determined by atoms up to the third layer, the *A* and *B* spectra of the ion scattering are the same. This cell has

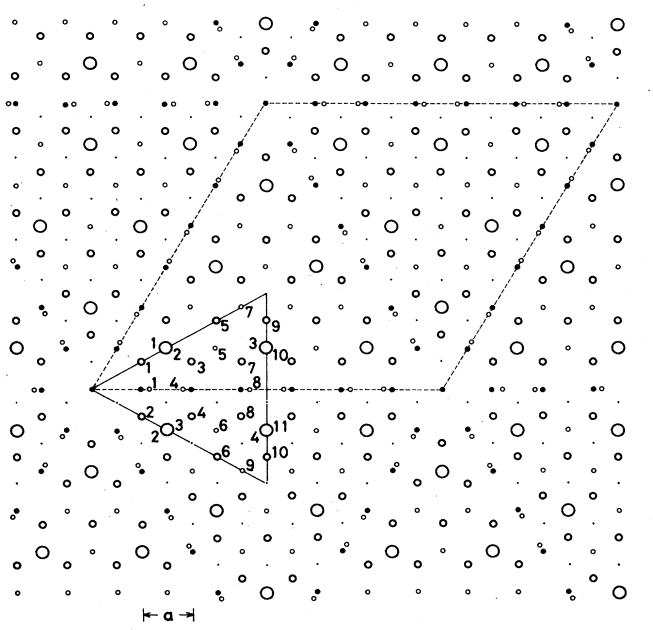

FIG. 5. The same for the adatom stacking-fault model (ASM) as in Fig. 1. The fourth-, sixth-, and eighth-layer atoms are hidden behind the third-, fifth-, and seventh-layer atoms, respectively. There are also the third-layer atoms behind the first-layer atoms. In the upper and lower halves of our unit cell, there are also the fifth- and seventh-layer atoms, respectively, behind the second-layer atoms. The solid circles show the fourth-layer atoms which are not behind the third-layer atoms and on the sides and the shift diagonal of the real unit cell. The third-layer atoms behind the first-layer atoms in the reconstructed ASM remain where they are in the unreconstructed ASM.

TABLE VI. The same for the adatom stacking-fault model (ASM) as Table IV.

		$\beta/\alpha=0.29$			$\beta/\alpha=0.4$		
Layer	Atom	Magnitude	Polar angle (deg)	Azimuthal angle (deg)	Magnitude	Polar angle (deg)	Azimuthal angle (deg)
1	1	0.18627a	2.42	−150.0*	0.18585a	2.37	−150.0*
	2	0.18727a	2.87	150.0*	0.18703a	2.73	150.0*
	3	0.18764a	0.31	90.0*	0.18667a	0.29	90.0*
	4	0.18856a	0.30	−90.0*	0.18781a	0.40	−90.0*
2	1	0.07204a	29.3	30.0*	0.07562a	32.4	30.0*
	2	0.07112a	29.1	−30.0*	0.07526a	32.1	−30.0*
	3	0.09284a	38.3	−171.6	0.09584a	40.6	−174.3
	4	0.09414a	38.0	171.5	0.09689a	40.3	174.7
	5	0.08020a	17.3	−150.0*	0.08391a	15.1	−150.0*
	6	0.08695a	14.9	150.0*	0.09063a	12.8	150.0*
	7	0.09136a	35.8	−5.76	0.09403a	38.1	−3.07
	8	0.09192a	35.7	5.91	0.09505a	37.8	2.67
	9	0.08377a	30.7	−90.0*	0.08602a	34.0	−90.0*
	10	0.08323a	31.1	90.0*	0.08573a	34.2	90.0*
3	1	0.04051a	23.1	179.0	0.04030a	24.1	179.6
	4	0.04921a	41.4	179.9	0.04946a	38.4	−179.7
	5	0.08896a	20.8	−90.0	0.09128a	18.4	−90.0
	6	0.09306a	18.1	90.0	0.09579a	15.5	90.0
	7	0.08512a	8.57	−150.0*	0.09068a	9.30	−150.0*
	8	0.04000a	18.7	0.82	0.04282a	16.4	−0.68
	9	0.08600a	9.26	150.0*	0.09165a	9.93	150.0*

the smallest number, 19, of dangling bonds among the models discussed.

The magnitude and direction of the shift of atoms are given in Table VI. Adatoms shift almost upward by about 90% of the layer distance. However, as four inequivalent adatoms shift by an almost equal amount, this model cannot explain the difference in the heights of adatoms on the two halves of the cell. Table II shows that the bond length of surface atoms is larger than that of the bulk l. Our calculation shows that near the rebonded pair of the unreconstructed ASM, there are six bonds with length 1.036l and a bond with length 1.089l. In the reconstructed ASM the former has length 1.028l—1.059l and 1.026l—1.063l for $\beta/\alpha=0.29$ and 0.4, respectively,

TABLE VII. The same for ASM as Table III.

Layer	Unreconstructed (deg)	Number of bonds	$\beta/\alpha=0.29$ (deg)	$\beta/\alpha=0.4$ (deg)
1-2-3	123.75	(2 + 4)×6	125.0—126.5	125.1—126.4
	108.76	(4 + 2)×6	116.0—118.7	116.5—119.1
	38.94	3×12	57.72—58.34	58.16—58.77
2-1-2	109.47	3×12	91.66—100.3	91.37—100.1
2-3-2	130.93	2×9	127.7—132.9	128.7—133.2
	109.47	3×30	95.56—118.9	95.18—119.6
2-3-3	105.23	4×9	100.7—103.0	100.1—102.4
2-3-4	109.47	3×30	106.2—117.6	106.4—117.9
	103.97	4×9	107.4—108.4	107.6—108.4
3-2-3	133.60	6	124.9—125.0	124.1—124.2
	122.42	2×4×3	115.2—116.9	115.0—116.7
	109.47	3×20	107.1—113.9	107.2—113.5
	96.15	4×9	95.88—96.75	96.48—97.32
3-3-4	105.23	2×9	102.6—106.5	102.8—106.0
3-4-5	122.42	2×9	119.3—122.3	118.8—121.6
	109.47	3×30	106.4—113.3	106.1—113.0
	108.76	2×9	110.7—111.0	110.4—110.6
	96.15	2×9	99.55—101.9	99.89—102.0

and the latter has length $1.047l-1.062l$ and $1.049l-1.065l$. Bond angles are given in Table VII. The reconstructed ASM has nearly mirror symmetry with respect to the borders of the triangular subunit.

As shown in Tables VI and VII, the atomic arrangement of the reconstructed ASM is nearly independent of β/α. Physically, the reconstruction is almost uniquely determined because the rebonding of the third-layer atoms along the stacking faults is so strong.

Figure 6 shows the ion scattering spectra. The unreconstructed ASM does not explain the experiment.[2] Here, the A and B spectra have big jumps at around 12°, 16°, 26°, and 45°, and the C spectrum has jumps at around 11°, 14°, 18°, and 40°. For the A and B spectra, nine adatoms and eight second-layer atoms are visible at angles below 12°. The remaining three adatoms, 18 second- and four third-layer atoms become visible at 12°, seven second- and two third-layer atoms at around 16°, three second- and 37 third-layer atoms at around 26°, and six second- and 21 third-layer atoms at around 45°. For the C spectrum, six adatoms and four second-layer atoms are visible at angles below 11°. The remaining six adatoms and two second-layer atoms become visible at 11°, six second- and two third-layer atoms at 14°, 30 second-, and 32 third-layer atoms at around 18°, and 15 third-layer atoms at around 40°. The fourth-layer atoms become visible at around 35° for the A and B spectra, resulting in small jumps at those angles.

The reconstructed ASM, nearly independently of β/α, gives spectra close to those of the pyramidal model. The C spectrum of this model is the closest to that of the pyramidal model among the models discussed in this paper. This is the main advantage of the ASM. Recall that the criticism of the AM by Aono *et al.*[2] is that the unreconstructed AM cannot explain the strong intensity of the C spectrum at relatively low angles, 10°—17°. The reconstructed AM improves the spectra, but it is not completely satisfactory.

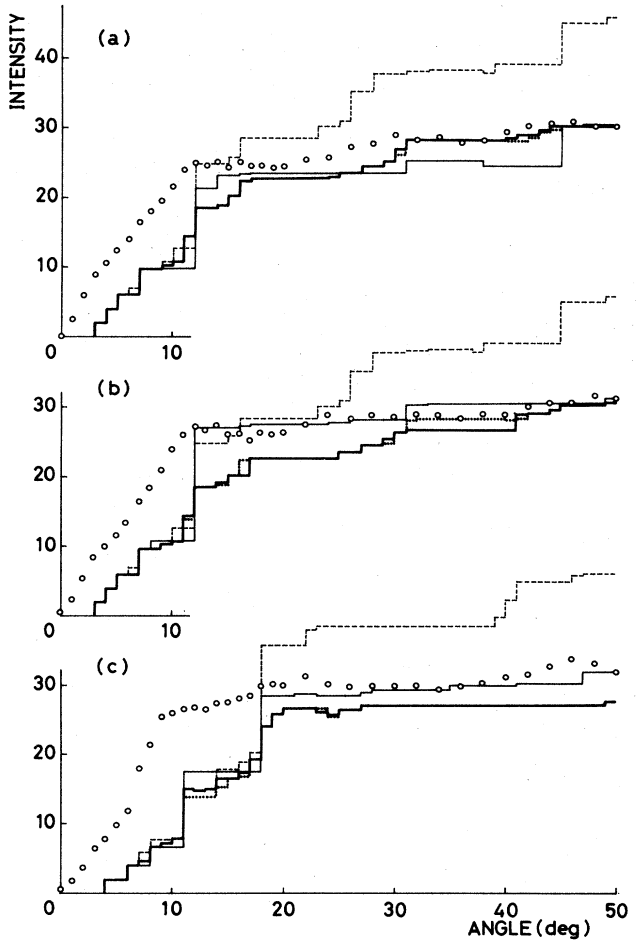

FIG. 6. The same for ASM as in Fig. 2.

D. The adatom stacking-fault π-bond model

We show the atomic displacement and the ion scattering spectra of the adatom stacking-fault π-bond model in Fig. 7. The shift of atoms and the bond angles are given in Tables VIII and IX, respectively. The rebonding creates a larger shift for adatom 4 than for others. If we take into account the fact that atoms near a deep hole have apparently stronger scanning tunneling spectra, we can explain the difference in the heights of adatoms on the two halves of the cell. The reconstructed structure is

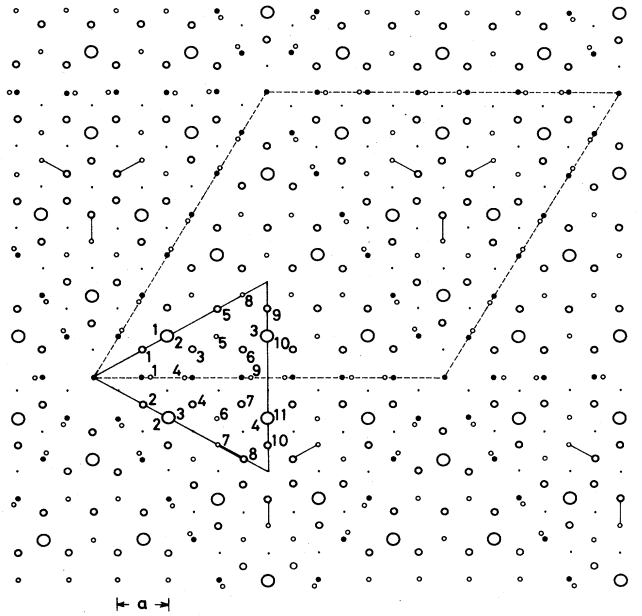

FIG. 7. The same for the adatom stacking-fault π-bond model (ASPM) as in Fig. 1. Atomic arrangement is the same as that of ASM in Fig. 5 except for the reversal of bonding of the second-layer atom 6 of ASM and the third-layer atom 9. This rebonding is shown schematically by the segmented lines. The second-layer atom 5 in this figure and the third-layer atom 8 can be also rebonded, but this is not taken into account in order to explain the difference in the heights of adatoms on the two halves of the unit cell (see text). The third-layer atoms behind the first-layer atoms in the reconstructed ASPM remain where they are in the unreconstructed ASPM.

TABLE VIII. The same for the adatom stacking-fault π-bond model (ASPM) as Table IV.

		$\beta/\alpha=0.29$			$\beta/\alpha=0.4$		
Layer	Atom	Magnitude	Polar angle (deg)	Azimuthal angle (deg)	Magnitude	Polar angle (deg)	Azimuthal angle (deg)
1	1	0.18820a	2.09	−150.0*	0.18697a	1.79	−150.0*
	2	0.18089a	6.54	−30.0*	0.17990a	7.15	−30.0*
	3	0.19122a	0.06	90.0*	0.18691a	0.19	90.0*
	4	0.22933a	12.4	90.0*	0.22639a	12.1	90.0*
2	1	0.07436a	28.6	30.0*	0.07733a	31.8	30.0*
	2	0.08696a	31.4	−30.0*	0.08908a	34.6	−30.0*
	3	0.09339a	37.5	−167.8	0.09420a	39.8	−170.8
	4	0.06925a	33.9	−157.4	0.07175a	38.0	−157.1
	5	0.08377a	17.0	−150.0*	0.08255a	15.7	−150.0*
	6	0.09184a	35.4	−5.75	0.09202a	38.5	−3.15
	7	0.08405a	38.5	8.49	0.08587a	42.2	6.50
	8	0.26274a	6.71	150.0*	0.26151a	7.18	150.0*
	9	0.08588a	30.1	−90.0*	0.08534a	33.9	−90.0*
	10	0.16935a	23.9	90.0*	0.16858a	24.6	90.0*
3	1	0.04407a	13.5	−157.6	0.04132a	15.7	−159.8
	4	0.04581a	32.0	−157.4	0.04277a	31.3	−157.9
	5	0.08977a	20.7	−90.0	0.08776a	19.3	−90.0
	6	0.05634a	22.0	−8.71	0.05503a	24.5	−8.94
	7	0.12790a	78.7	−30.0*	0.13075a	76.1	−30.0*
	8	0.08710a	8.49	−150.0*	0.08719a	9.77	−150.0*
	9	0.03446a	20.7	15.5	0.03243a	20.7	18.0

TABLE IX. The same for ASPM as Table III.

Layer	Unreconstructed (deg)	Number of bonds	$\beta/\alpha=0.29$ (deg)	$\beta/\alpha=0.4$ (deg)
1-2-2	118.13	2×3	114.1	114.1
1-2-3	123.75	(2 + 4)×6−2×3	123.4−126.7	123.4−126.6
	108.76	(4 + 2)×6	115.2−118.8	116.0−119.3
	38.94	3×12	56.88−62.11	57.17−62.35
2-1-2	109.47	3×12	91.24−100.8	90.54−100.5
2-2-2	120	6	122.9	122.9
2-2-3	118.13	2×6	100.9−122.3	101.1−122.3
2-3-2	130.93	2×9	128.9−132.8	129.5−133.0
	109.47	3×30−7×3	95.6−118.6	95.5−119.0
2-3-3	118.13	4×3	111.1−123.2	110.7−122.5
	105.23	4×9	100.1−104.1	99.63−103.4
2-3-4	109.47	3×30−5×3	105.9−124.9	105.8−124.8
	103.97	4×9	106.7−109.0	106.9−109.1
	66.16	3	100.1	100.8
3-2-3	133.60	6	123.9−126.1	123.0−125.1
	122.42	4×6	114.8−118.4	114.5−117.5
	109.47	3×10+2×6	103.4−113.7	103.5−113.4
	96.15	4×9	94.48−97.37	95.01−98.03
3-3-3	120	3	104.2	104.3
3-3-4	105.23	2×9	102.8−105.8	102.7−105.5
	90	2×3	89.76	90.74
3-4-5	152.78	3	140.2	138.8
	122.42	2×9	119.6−121.7	119.2−121.1
	109.47	3×30−3×3	107.3−112.4	107.6−112.2
	108.76	2×9	110.4−111.9	110.2−111.3
	96.15	2×9	99.70−101.8	99.73−101.7
	85.36	2×3	98.36	98.85

almost independent of β/α. The ion scattering spectra are shown in Fig. 8. While the spectra of the unreconstructed structure is far from those of the pyramidal model, the spectra of the reconstructed structure is close to those of the pyramidal model.

E. The adatom double-stacking-fault model

Bennet[7] proposed the model shown in Fig. 9. There are double-layer stacking faults along the border of a triangular subunit. The first-layer atoms are at the *A* site. The second-, third-, and fourth-layer atoms are at the *B*, *C*, and *C* sites for the lower-left half of the unit cell, and at the *C*, *B*, and *B* sites for the upper-right half. From the fifth layer, atoms are at the *A*, *A*, *C*, *C*, *B*, and *B* sites for either half of the cell. Pairs of neighboring atoms along the lines of stacking faults in the second layer rebond with each other. Similarly, the fifth-layer atoms on the lines of stacking faults shift laterally and rebond with each other. The arrangement of the first- through sixth-layer atoms has mirror symmetry with respect to any border of the triangular subunit. The unit cell has 33 dangling bonds.

Tables X and XI show the calculated atomic displacement and bond angles, respectively. The arrangement of atoms in the reconstructed ADM has no mirror symmetry with respect to any border of the triangular subunit. Atoms near the corner of the cell with a deep hole have a large shift from the positions of the unreconstructed ADM. Figure 10 shows the ion scattering spectra. Those of the reconstructed ADM and the pyramidal model are close to each other.

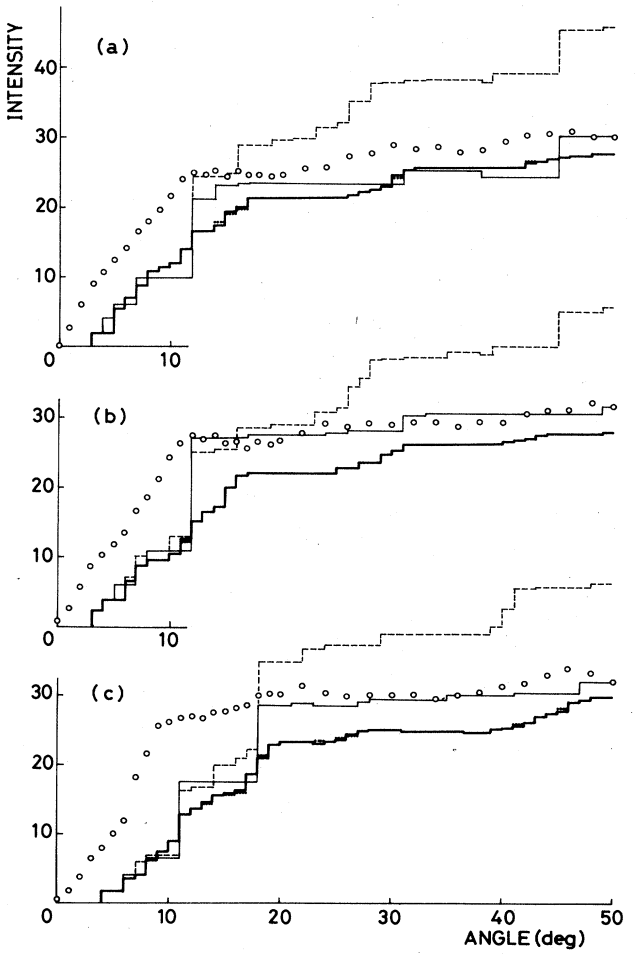

FIG. 8. The same for ASPM as in Fig. 2.

F. Concluding remark

We have investigated the reconstructed structure of five adatom-related models which are consistent with scanning tunneling microscopy and compared the calculated and observed ion scattering spectra. The unreconstructed structures of all models do not explain experiment[2] very well. The reconstructed structures give improved spectra. They are close to those of the pyramidal model. The reconstructed ASM gives perhaps the best ion scattering spectra. However, as the reconstructed structures of all models give similar spectra, we cannot really determine the best model using only ion scattering spectroscopy. This is because the observed spectra have broad peaks.

III. DISCUSSION

A. The π-bond chain model of Si(111)2×1 structure by the Keating model

Upon cleaving Si(111) at room temperature, a metastable multidomain 2×1 structure is obtained.[12] Upon an-

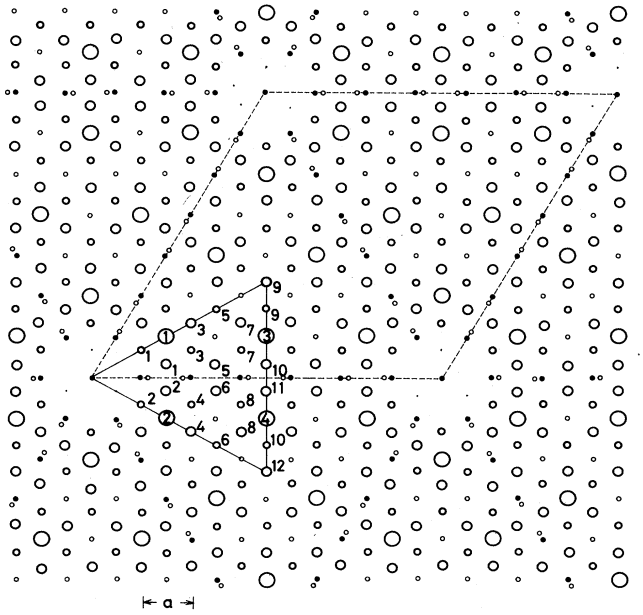

FIG. 9. The same for the adatom double-stacking-fault model (ADM) as in Fig. 1. The solid circles show the sixth-layer atoms which are not behind the fifth-layer atoms. All atoms in the reconstructed ADM shift from the positions where they are in the unreconstructed ADM.

TABLE X. The same for the adatom double-stacking-fault model (ADM) as Table IV.

			$\beta/\alpha=0.29$			$\beta/\alpha=0.4$	
Layer	Atom	Magnitude	Polar angle (deg)	Azimuthal angle (deg)	Magnitude	Polar angle (deg)	Azimuthal angle (deg)
1	1	0.18068a	22.6	−150.0*	0.18514a	24.3	−150.0*
	2	0.18638a	1.19	150.0	0.18906a	1.39	150.0*
	3	0.16413a	4.91	−90.0*	0.17205a	5.14	−90.0*
	4	0.16594a	5.03	90.0*	0.17212a	5.02	90.0*
2	1	0.07404a	13.1	31.7	0.07529a	14.1	26.3
	2	0.08553a	30.8	−121.3	0.08531a	30.8	−119.0
	3	0.10394a	62.9	−150.0*	0.10962a	62.7	−150.0*
	4	0.07854a	55.7	150.0*	0.08235a	56.3	150.0*
	5	0.04869a	11.8	89.7	0.03889a	11.4	90.0
	6	0.05022a	23.1	−116.9	0.04223a	25.0	−117.7
	7	0.06946a	48.6	−50.1	0.07541a	49.0	−49.1
	8	0.07081a	49.8	46.0	0.07549a	50.5	44.6
	9	0.03747a	0.0*	0.0*	0.03385a	0.0*	0.0*
	10	0.07874a	0.0	0.0	0.07920a	0.0	0.0
	11	0.07899a	0.0	0.0	0.07974a	0.0	0.0
	12	0.03183a	0.0*	0.0*	0.02700a	0.0*	0.0*
3	1	0.04470a	15.5	30.0*	0.04865a	13.5	30.0*
	2	0.04341a	76.4	150.0*	0.04213a	76.3	150.0*
	3	0.04039a	83.9	−87.7	0.04290a	85.7	−88.8
	4	0.03061a	69.0	119.8	0.02966a	72.9	118.5
	5	0.12834a	12.9	−150.0*	0.13539a	12.5	−150.0*
	6	0.12331a	5.51	150.0*	0.12925a	5.27	150.0*
	7	0.03894a	71.7	−87.1	0.04025a	74.5	−87.6
	8	0.03798a	69.9	89.6	0.03863a	72.5	89.4
	9	0.01694a	13.6	90.0*	0.01546a	8.45	90.0*
	10	0.01274a	15.3	−90.0*	0.01062a	10.9	−90.0*

TABLE XI. The same for ADM as Table V.

Layer	Unreconstructed (deg)	Number of bonds	$\beta/\alpha=0.29$ (deg)	$\beta/\alpha=0.4$ (deg)
1-2-2	160.53	2×9	148.9—152.8	148.6—152.3
1-2-3	180.0	(1 + 2)×6	157.4—160.9	156.7—160.6
	70.53	6×12	80.65—88.39	81.12—89.34
2-1-2	109.47	3×12	92.26—108.3	91.64—109.0
2-2-3	118.13	4×15	108.5—116.3	108.4—116.1
2-3-2	109.47	1×6+3×36	94.10—117.0	93.88—117.2
2-3-4	109.47	2×6+3×36	100.2—115.7	100.7—116.0
3-2-3	109.47	30 + 3×20	105.0—117.1	104.9—117.1
3-4-5	109.47	3×42−4×9	105.2—112.6	105.3—113.5
	108.76	4×9	106.6—111.2	106.7—111.0
4-5-5	105.23	4×9	102.7—106.3	102.2—105.5
4-5-6	109.47	3×42−4×9	106.5—113.9	106.4—113.2
	103.97	4×9	104.5—106.5	105.0—106.9
5-4-5	133.60	6	128.1—131.8	127.0—130.5
	122.42	4×6	121.0—124.3	119.9—122.8
	109.47	3×42−5×6−4×9	104.6—116.1	105.0—115.1
	96.15	4×9	98.38—100.4	99.05—101.0
5-5-6	105.23	2×9	101.7—107.4	101.7—106.6

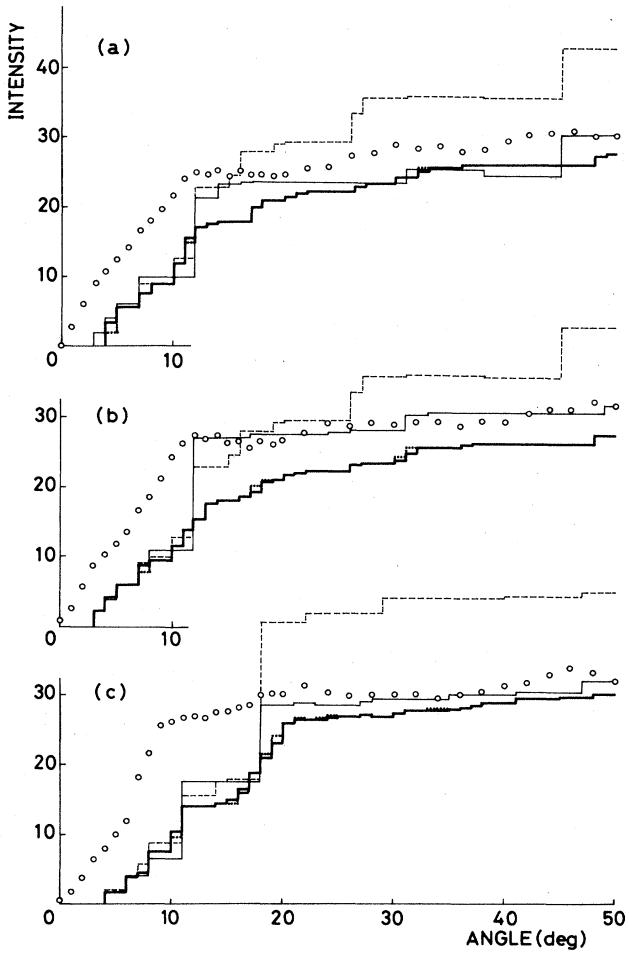

FIG. 10. The same for ADM as in Fig. 2.

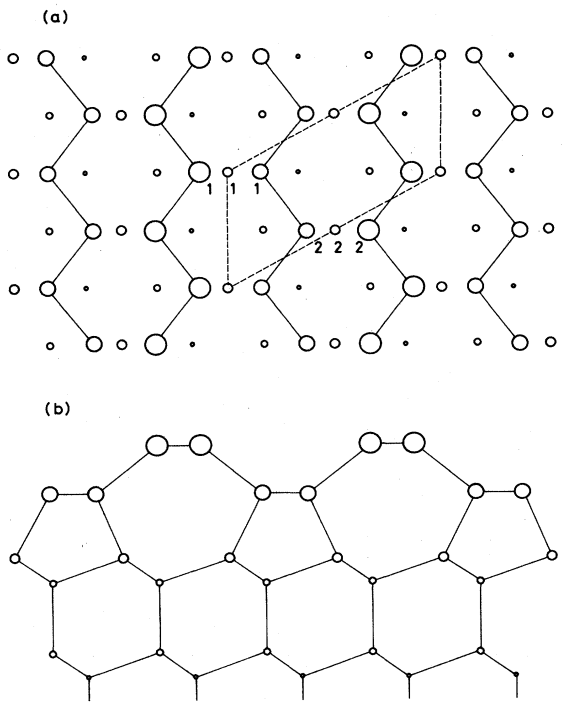

FIG. 11. The 2×1 unit cell of the π-bond chain model of the *reconstructed* Si(111)2×1 structure. (a) Top view. The first-, second-, third-, fourth-, and sixth-layer atoms are denoted by circles with diameters which are smaller for deeper atoms. The fifth-, seventh, and eighth-layer atoms are hidden behind the fourth-, sixth-, and third-layer atoms, respectively. The first- and second-layer atoms shift from the lattice sites to the direction of azimuthal angle 150°, as shown in Table XII. Here, the coordinate system is rotated by 30° with respect to the axis which penetrates the lower-left corner of the cell and is perpendicular to the surface. (b) Side view.

nealing to about 500 K, the 2×1 structure irreversively transforms to a 7×7 structure, which in turn transforms reversively to a 1×1 structure upon further heating to about 1170 K.

Pandey[11] performed a self-consistent pseudopotential calculation on an ideal Si(111)2×1 surface and proposed the π-bond chain model shown in Fig. 11. A first-layer atom is rebonded to a third-layer atom and becomes a second-layer atom with fourfold coordination. Then a neighboring atom in the second layer becomes a first-layer atom with threefold coordination. As a result, the dangling-bond orbitals get close enough to interact significantly and cause a substantial reduction of the total energy.

The Keating model[8] is valid for calculating atomic dis-

TABLE XII. The same for the π-bond chain model of the Si(111)2×1 structure as Table IV.

			$\beta/\alpha=0.29$			$\beta/\alpha=0.4$	
Layer	Atom	Magnitude	Polar angle (deg)	Azimuthal angle (deg)	Magnitude	Polar angle (deg)	Azimuthal angle (deg)
1	1	0.28931a	54.4	147.6	0.32146a	48.7	149.9
	2	0.34137a	61.7	148.1	0.38663a	56.8	149.9
2	1	0.31089a	87.4	148.3	0.33106a	86.5	149.9
	2	0.22399a	89.0	147.4	0.23379a	86.1	149.9
3	1	0.02573a	57.1	−24.2	0.02533a	39.3	−29.9
	2	0.04280a	23.9	90.0	0.04736a	21.2	150.0

placements away from the surface but may not be completely justified for the surface atoms. To check the reliability of our calculation, we also obtained the atomic displacement and ion scattering spectra of the π-bond model of the Si(111)2×1 structure within the framework of the Keating model. Tables XII and XIII show the shift of atoms and bond angles, respectively. All the first- and second-layer atoms shift to the direction of azimuthal angle 150°. The lateral components of shifts of the first-layer atoms are $0.2354a-0.3005a$ for $\beta/\alpha=0.29$. The second-layer atoms shift almost laterally by $0.2240a-0.3106a$, but deeper atoms shift only slightly. The resultant atomic arrangement shown in Fig. 11 is similar to that of Pandey.[11]

As in Secs. II B and II D, near the rebonded pair of the unreconstructed structure there are four bonds with length $0.943l$ and a bond with length $1.374l$. In the reconstructed structure, the former has length $1.000l-1.022l$ and $1.016l-1.031l$ for $\beta/\alpha=0.29$ and 0.4, respectively, and the latter has the length $1.078l$ and $1.070l$.

Table I shows that the strain energies of the reconstructed structures are about 80%, 60%, 80%, 70%, 75%, and 23% of those of the unreconstructed ones of AM, APM, ASM, ASPM, and ADM, and the 2×1 model, respectively. This means that the 2×1 model is easily reconstructed in comparison to the 7×7 models, whose surfaces are capped with adatoms. Figure 12 shows the ion scattering spectra of the 2×1 model.

B. Change of bond stretching constants

So far, we have obtained reconstructed structures of several models, setting the bond-stretching constant to be the value of the bulk,[8] 38.71 eV/cell. In general, the bond interaction of surface atoms is different from that of the bulk. If the surface is softened, the strain energy in Table I should be multiplied by the ratio of interaction constants of the surface to the bulk α/α_0 which is less than 1.

Among the surface electronic energies we only take into account the energy cost of bond cutting and the energy benefit of the π bonding, leaving the full-scale calculation of the electronic energy for future work. The energy cost of cutting a bond is around 2.4 eV (Refs. 9 and 13) and the energy benefit of rebonding a pair of atoms is 0.56 eV (Ref. 11). We assume that the bond-cutting and π-

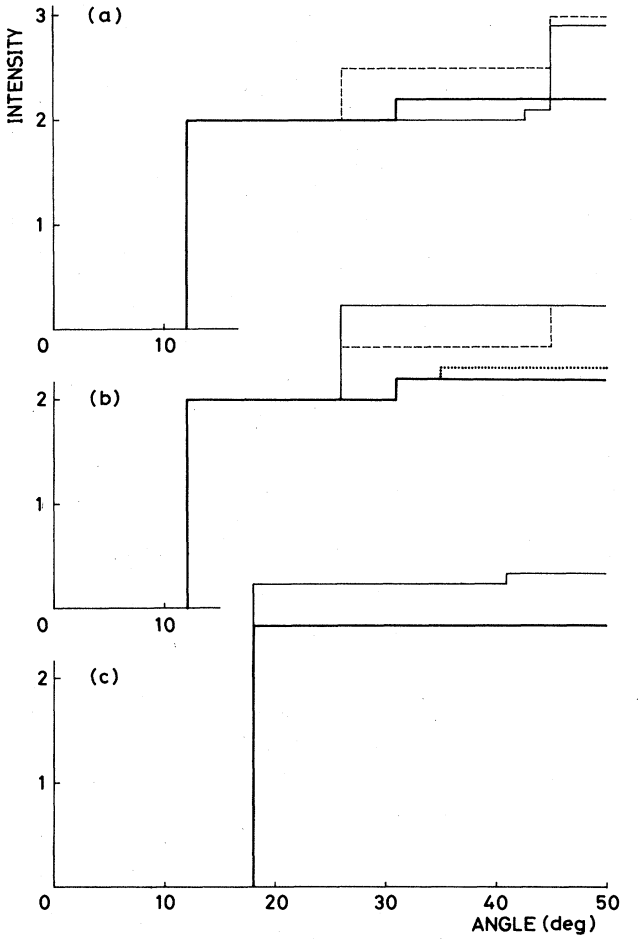

FIG. 12. The ion scattering spectra for the π-bond chain model of the Si(111)2×1 structure. The dotted, thick solid, dashed, and thin solid lines show the spectra of the reconstructed structures for $\beta/\alpha=0.29$ and 0.4, the unreconstructed structure, and the ideal 1×1 structure, respectively. (a) The azimuthal angle of the ion direction of incidence is along the $[\bar{2}11]$ direction. The spectra of the reconstructed structures for $\beta/\alpha=0.29$ and 0.4 are the same. (b) The azimuthal angle is along the $[2\bar{1}\,\bar{1}]$ direction. (c) The azimuthal angle is along the $[01\bar{1}]$ and $[0\bar{1}1]$ directions. The spectra of the reconstructed structures for $\beta/\alpha=0.29$ and 0.4 are the same. Those of the unreconstructed and ideal structures are also the same.

TABLE XIII. The same for the π-bond chain model of the Si(111)2×1 structure as Table V.

Layer	Unreconstructed (deg)	Number of bonds	$\beta/\alpha=0.29$ (deg)	$\beta/\alpha=0.4$ (deg)
1-1-1	120	2	109.4	106.9
1-1-2	118.13	4	117.6–118.3	117.5
1-2-2	118.13	4	118.4–120.0	117.9–118.6
1-2-3	109.47	1	105.5	109.1
	66.16	1	103.7	108.4
2-2-2	120	2	106.2	104.7
2-2-3	110.06	2	101.5–102.5	102.1
	90	2	102.7–103.4	102.6
2-3-4	152.79	1	127.0	126.2
	109.47	3	92.71–117.7	93.61–117.4
	85.36	2	99.28–100.3	100.7

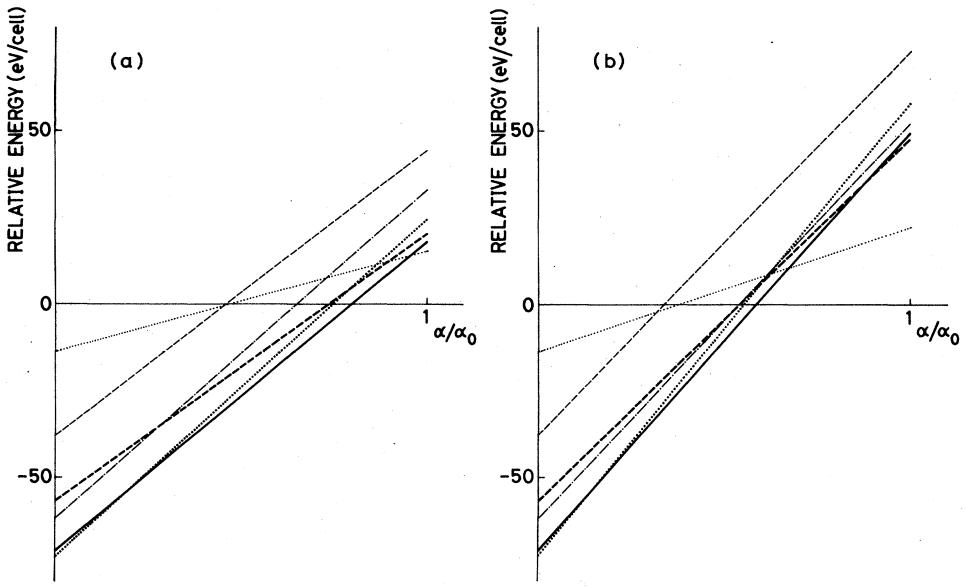

FIG. 13. Dependence of the energy per 7×7 unit cell on the ratio of the bond-stretching constants of the surface to the bulk α/α_0. Energy is measured relative to that of an ideal surface with 49 dangling bonds in the cell. Thick dashed, chain, thick solid, thick dotted, thin dashed, and thin dotted lines show the energies of the reconstructed AM, APM, ASM, ASPM, ADM, and Si(111)2×1 models, respectively. The energies of the unreconstructed structures of the above models are equal to those of the corresponding reconstructed ones for $\alpha/\alpha_0=0$ and have slopes steeper than those of the reconstructed ones for $\alpha/\alpha_0\neq0$. Note that the relative energy of the pyramidal model (Ref. 2) is 113.8 eV/cell, independent of both α/α_0 and β/α, and higher than the energies of any models discussed in this paper. Note also that the relative energy of the adatom triangle-dimer model (Ref. 4) is 56.9 (and more) eV/cell for $\alpha/\alpha_0=0$ and $\alpha/\alpha_0\neq0$, respectively, and higher than the energies of models discussed in this paper. (a) $\beta/\alpha=0.29$. (b) $\beta/\alpha=0.4$.

bonding energies are proportional to the numbers of dangling bonds and π bonds in the unit cell, respectively.

Figure 13 shows the α/α_0 dependence of the surface energy for the reconstructed structures of models described above. Here, we set to zero the energy of the ideal truncated 7×7 model with 49 dangling bonds in the unit cell. The energy of 7×7 primitive cells is plotted for the Si(111)2×1 structure. For $\beta/\alpha=0.29$ the model with the lowest energy is the ideal model if $0.8\lesssim\alpha/\alpha_0$ and the ASM if $0.2\lesssim\alpha/\alpha_0\lesssim0.8$. For $\beta/\alpha=0.4$ the energy of the AM is lower than that of the ASM but higher than that of the ideal model if $0.85\lesssim\alpha/\alpha_0$. The ideal model and the ASM have the lowest energy for $0.6\lesssim\alpha/\alpha_0$ and $0.2\lesssim\alpha/\alpha_0\lesssim0.6$, respectively. When the 2×1 model has lower energy than the ideal 1×1 model, it has higher energy than the 7×7 models. This explains the experimental fact that the 2×1 structure irreversibly transforms to the 7×7 structure.[12]

The energy consideration above shows that the reconstructed ASM is the best model of the 7×7 structure among those discussed in this paper, and that the surface is softened, if the 7×7 structure has lower energy than the ideal structure.

ACKNOWLEDGMENTS

The author thanks Professor A. Ichikawa for a critical reading of the manuscript. He also thanks Professor K. Takayanagi and Dr. E. G. McRae for communicating experimental data prior to publication. The computations were performed at the Computer Center of the Institute of Molecular Science, Okazaki 444, Japan, using the computer subroutine STEPIT (copyright 1965, J. P. Chandler, Physics Department, Indiana University).

[1]G. Binnig, H. Rohrer, Ch. Gerber, and E. Weibel, Phys. Rev. Lett. **50**, 120 (1983); G. Binnig, H. Rohrer, F. Salvan, Ch. Gerber, and A. Baro (unpublished).

[2]M. Aono, R. Souda, C. Oshima, and Y. Ishizawa, Phys. Rev. Lett. **51**, 801 (1983).

[3]T. Yamaguchi, Phys. Rev. B **30**, 1992 (1984).

[4]E. G. McRae and P. M. Petroff, Surf. Sci. (to be published).

[5]K. Takayanagi, Y. Tanishiro, S. Takahashi, and K. Yagi, J. Vac. Sci. Technol. (to be published).

[6]D. J. Chadi (unpublished).

[7]P. A. Bennet, F. Comin, J. E. Rowe, and P. H. Citrin, Bull. Am. Phys. Soc. **28**, 532 (1983).

[8]P. N. Keating, Phys. Rev. **145**, 637 (1966).

[9]T. Yamaguchi, Phys. Rev. B **31**, 5297 (1985).

[10]The 13 second-layer atoms which do not shift are the dangling-bond-site atoms. The strain is small in a region near the dangling-bond-site atom. In Ref. 9 we considered the equilateral triangular region with a side of $2a$ where the strain

is large. There is an adatom at the center of the triangle. The 27 third-layer atoms which do not shift are located at the center of the side of the triangle and in the nearest neighbor of the dangling-bond-site atom.

[11]K. C. Pandey, Phys. Rev. Lett. **47**, 1913 (1981); **49**, 223 (1982).
[12]D. E. Eastman, J. Vac. Sci. Technol. **17**, 492 (1980).
[13]L. C. Snyder, Z. Wasserman, and J. W. Moskowitz, J. Vac. Sci. Technol. **16**, 1266 (1979).